Modeling of a constant Q: Methodology and algorithm for an efficient and optimally inexpensive viscoelastic technique

Joakim O. Blanch* **Johan O. A. Robertsson†** **William W. Symes‡**

Abstract

Linear anelastic phenomena in wave propagation problems can be well modeled through a viscoelastic mechanical model consisting of standard linear solids. In this paper we present a method for modeling of constant Q as a function of frequency based on an explicit closed formula for calculation of the parameter fields. The proposed method enables substantial savings in computations and memory requirements. Experiments show that the new method also yields higher accuracy in the modeling of Q than e.g., the Padé approximant method [7].

1 Introduction

Earth media attenuate and disperse propagating waves. Several modeling methods for wave propagation, which take attenuating and dispersive effects into account, have been presented (e.g., Robertsson et al. [16], Carcione et al. [5], and Martinez and McMechan [11]) as have inversion methods developed for viscoelastic media (e.g., Blanch and Symes [1] and Martinez and McMechan [12]). Attenuating effects also have a large impact on AVO results [13].

Attenuating and dispersive effects are often quantified by the "quality factor", Q. This quantity is losely defined as the number of wavelengths a wave can propagate through a medium before its amplitude has decreased by $e^{-\pi}$. A more strict definition of Q will be given in the following section. Q has been found to be essentially constant as a function of frequency [14] over the seismic frequency range, (approximately 1-200 Hz). Therefore a wave of higher frequency propagates a shorter *distance* to decay a certain amount in amplitude, compared to a wave of lower frequency. Futterman [8] showed, through Kramer-Krönig's relation, that a constant Q implied a specific dispersion relation. This dispersion relation was showed to hold for both shale and plexiglass by Wuenchel [19].

A correct modeling scheme should thus yield a constant Q and the dispersion relation prescribed by Futterman [8]. This is easily obtained for a modeling method based in the frequency domain, but is slightly more cumbersome for modeling methods based in the time domain. Modeling methods based in the frequency domain are essentially limited to 1-D or layered (through propagator

*The Rice Inversion Project, Department of Gology and Geophysics, Rice University, Houston TX 77251-1892

†Department of Geology and Geophysics, Rie University, Houston TX 77251-1892

‡The Rice Inversion Project, Department of Computational and Applied Mathematics, Rice University, Houston TX 77251-1892

matrices) media and we will therefore focus on "time domain methods". An approximately constant Q is usually constructed, by using simple viscoelastic building blocks, to obtain a numerically efficient modeling method based in the time domain. Day and Minster [7] showed that the best Padé approximant to a constant Q is a so-called Standard Linear Solid (SLS). Day and Minster [7] also described a method to connect several SLSs in parallel to yield an excellent approximation to a constant Q in a pre-defined frequency band. The method requires several SLSs to yield a good result and each SLS is described by an individual parameter set. These two drawbacks makes the approximation method expensive, with respect to both memory and time, to use for viscoelastic wavepropagation modeling methods. The method is also quite complicated, since it for instance is necessary to find roots of Legendre polynomials.

In this paper we present a method to find approximations to a constant Q which is easier to use than Day and Minster's [7] method and yields good approximations using only a few SLSs. The viscoelastic description, used in the method, yields savings during the viscoelastic wave simulation as well. We have chosen to call the method, the "τ-method", after the notation used in deriving the algorithm.

We will start by reviewing some basic viscoelastic concepts and definitions. We will then continue by describing our method and finally compare results from finite-difference viscoelastic wave propagation simulations, where the attenuation model was found using the τ-method, a single SLS approximation, the "Padé approximant" method [7], and an essentially analytic solution based on results from McDonal et al. [14], Futterman [8], and Wuenschel [19]. The analytic solution is obtained through a frequency domain method similar to the method described by Martinez and McMechan [11].

2 Linear Viscoelastic Model

The constitutive relation for a linear elastic 2-D $(i, j, k = x, y)$ or 3-D $(i, j, k = x, y, z)$ homogeneous solid is,

$$\sigma_{ij} = \lambda \varepsilon_{kk}\delta_{ij} + 2\mu\varepsilon_{ij}, \tag{2.1}$$

where σ_{ij} are the components of the stress tensor, λ and μ the Lamé constants, and ε_{ij} the components of the strain tensor. For a linear viscoelastic material the multiplications in equation (2.1) become convolutions and the Lamé constants time dependent, so that,

$$\sigma_{ij} = \dot{\Lambda} * \varepsilon_{kk}\delta_{ij} + 2\dot{\mathrm{M}} * \varepsilon_{ij}, \tag{2.2}$$

[6]. The dot denotes derivative in time. Thus, a current deformation state is related to previous ones through the stress relaxation functions, $\Lambda(t)$ and $\mathrm{M}(t)$. It is possible to express the time derivative of ε_{ij} as,

$$\dot{\varepsilon}_{ij} = \frac{1}{2}(\partial_i v_j + \partial_j v_i), \tag{2.3}$$

where v_i is the velocity. Let us define,

$$\Pi = \Lambda + 2\mathrm{M}. \tag{2.4}$$

Equations (2.2), (2.3), and (2.4) then yields,

$$\dot{\sigma}_{ij} = (\dot{\Pi} - 2\dot{\mathrm{M}}) * \partial_k v_k + \dot{\mathrm{M}} * \partial_i v_j. \tag{2.5}$$

Together with Newton's second law,

$$\dot{v}_i = \frac{1}{\rho}\partial_j \sigma_{ij}, \tag{2.6}$$

equation (2.5) describes viscoelastic wave propagation. The definition of $\Pi(t)$ allows us to independently define quality factors, Q, for P- and S-waves. Robertsson et al. [16] describe an efficient $O(2,4)$ finite-difference scheme to solve the problem.

The SLS (a spring and a dashpot in series in parallel with a spring) has been shown to be a quite general mechanical viscoelastic model (e.g., Day and Minster [7], Pipkin [15], and Blanch et al. [2]). An array of L SLS has the stress relaxation function,

$$\Gamma(t) = M_R \left(1 - \sum_{l=1}^{L}\left(1 - \frac{\tau_{\varepsilon l}}{\tau_{\sigma l}}\right) e^{-t/\tau_{\sigma l}}\right)\theta(t), \tag{2.7}$$

where $\theta(t)$ is the Heaviside function, M_R is the relaxed stress modulus corresponding to $\Gamma(t)$ [15], and $\tau_{\sigma l}$ and $\tau_{\varepsilon l}$ are the stress and strain relaxation times for the lth SLS [15]. With our formulation we therefore have,

$$\Pi(t) = \pi \left(1 - \sum_{l=1}^{L}\left(1 - \frac{\tau^p_{\varepsilon l}}{\tau_{\sigma l}}\right) e^{-t/\tau_{\sigma l}}\right)\theta(t), \tag{2.8}$$

and

$$\mathrm{M}(t) = \mu \left(1 - \sum_{l=1}^{L}\left(1 - \frac{\tau^s_{\varepsilon l}}{\tau_{\sigma l}}\right) e^{-t/\tau_{\sigma l}}\right)\theta(t), \tag{2.9}$$

where $\pi = \lambda + 2\mu$, and $\tau^p_{\varepsilon l}$ and $\tau^s_{\varepsilon l}$ are the strain relaxation times for P- and S-waves for the lth SLS. The same stress relaxation times, $\tau_{\sigma l}$, may be used for both P- and S-waves. In this paper, we will also refer to an SLS as a *relaxation mechanism*.

The complex stress modulus, $M_C(\omega)$, is defined as the Fourier transform of the stress relaxation function [15]. The quality factor, Q, is defined as,

$$Q(\omega) = \frac{Re(M_C(\omega))}{Im(M_C(\omega))} \tag{2.10}$$

[4]. Equation (2.10) defines Q as the number of wavelengths a pulse may propagate before its amplitude drops by a factor of $e^{-\pi}$ [18]. Q is thus generally a function of frequency. For an array of standard linear solids equations (2.7) and (2.10) yields,

$$Q(\omega) = \frac{1 - L + \sum_{l=1}^{L} \frac{1+\omega^2 \tau_{\varepsilon l}\tau_{\sigma l}}{1+\omega^2 \tau_{\sigma l}^2}}{\sum_{l=1}^{L} \frac{\omega(\tau_{\varepsilon l} - \tau_{\sigma l})}{1+\omega^2 \tau_{\sigma l}^2}} \tag{2.11}$$

We may thus express the viscoelastic medium in terms of two arrays of SLS, $\Pi(t)$ and $\mathrm{M}(t)$ (equations [2.8] and [2.9]), given the Q vs. frequency relations for P- and S-waves, the P- and S-velocities, and the density of the medium. Since attenuation and dispersion are related through Kramer-Krönig's relation [8], the choice of a physically realistic Q vs. frequency relation yields an equally physical dispersion relation. We will now derive a formula on closed form to calculate the $\tau_{\varepsilon l}$ and the $\tau_{\sigma l}$ in equation (2.11) for a desired constant Q, for P- and S-waves respectively.

3 The τ-method

The basic arguments for the τ-method are,

- simplicity in determining a constant Q model,
- memory savings and less calculations in forward modeling of viscoelastic waves,
- the convenience in having only one variable describing the magnitude of dispersion and attenuation in inversion routines.

We will later see that the τ-method also yields more accurate results at a low computational cost than e.g., the Padé approximant method. We will assume that we want to approximate a *constant* Q in a pre-defined frequency interval and that there exist L preset stress relaxation times, $\tau_{\sigma l}$ (see below).

The τ-method is based on the simple observation that the level of attenuation caused by a SLS can be determined by a dimensionless (frequency scale-independent) variable, τ. If we define τ as,

$$\tau = \frac{\tau_{\varepsilon l}}{\tau_{\sigma l}} - 1 = \frac{\tau_{\varepsilon l} - \tau_{\sigma l}}{\tau_{\sigma l}}, \tag{3.1}$$

the inverse of Q for one SLS can be written as,

$$Q^{-1} = \frac{\omega \tau_\sigma \tau}{1 + \omega^2 \tau_\sigma^2 (1+\tau)}. \tag{3.2}$$

It is easily seen that the behavior in frequency is essentially determined by τ_σ and the magnitude of Q for the SLS essentially by τ. This is not true for τ larger than, or even close to, 1. As we shall see, $\tau \ll 1$ generally. We have plotted Q as a function of frequency for a SLS with two diffferent τ_σ and two different τ in Figure 3.1, to illustrate the effect of the different parameters. The magnitude is the same but the curve is displaced in frequency when τ_σ is changed but τ remains constant. The magnitude of the curve changes with τ on the other hand, but the curve does not move in frequency

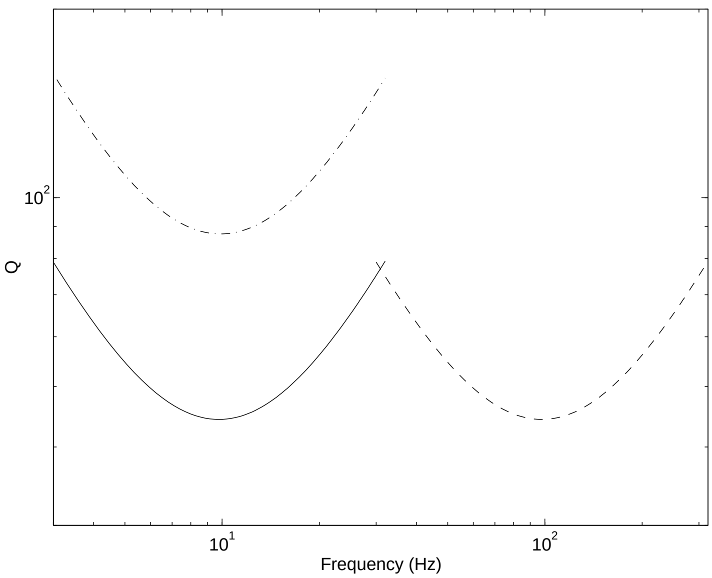

Figure 3.1: Q as a function of frequency for two different τ and two different τ_σ. Solid: $\tau = 4.6212 \times 10^{-2}$, $\tau_\sigma = 1.5915 \times 10^{-2}$ corresponds to 10 Hz. Dashed: $\tau = 4.6212 \times 10^{-2}$, $\tau_\sigma = 1.5915 \times 10^{-3}$ corresponds to 100 Hz. Dash-dotted: $\tau = 2.3106 \times 10^{-2}$, $\tau_\sigma = 1.5915 \times 10^{-2}$ corresponds to 10 Hz.

when τ_σ is held constant. We may therefore use τ as a means to determine the magnitude for several different SLSs, which assume maximum attenuation at different frequencies. For one SLS $\tau \approx 2Q_{min}^{-1}$, where Q_{min} is the global minimum for Q as a function of frequency. For more than one SLS, τ is even smaller. Q is rarely less than 20 for any real materials, implying that $\tau \ll 1$. Using the parameter τ to tune an array of SLSs, and assuming that $1 + \tau \approx 1$, equation (2.11) yields,

$$Q^{-1} \approx \sum_{l=1}^{L} \frac{\omega \tau_{\sigma l} \tau}{1 + \omega^2 \tau_{\sigma l}^2}. \tag{3.3}$$

In this (approximate) expression Q^{-1} is *linear* in τ. We can therefore easily find the best approximation in the least squares sense over a pre-defined frequency range to any Q_0, by minimizing over τ the expression,

$$J = \int_{\omega_a}^{\omega_b} \left(Q^{-1}(\omega, \tau_{\sigma l}, \tau) - Q_0^{-1} \right)^2 \, d\omega. \tag{3.4}$$

To find the minimum we set the derivative of J with respect to τ to zero, and solve for τ.

$$\frac{dJ}{d\tau} = 2\int_{\omega_a}^{\omega_b} \left(Q^{-1}(\omega,\tau_{\sigma l},\tau) - Q_0^{-1}\right) \frac{dQ^{-1}(\omega,\tau_{\sigma l},\tau)}{d\tau}\, d\omega = 0 \tag{3.5}$$

If we define,

$$F(\omega,\tau_{\sigma l}) = \sum_{l=1}^{L} \frac{\omega\tau_{\sigma l}}{1+\omega^2\tau_{\sigma l}^2}, \tag{3.6}$$

we can write equation (3.5) as,

$$\frac{dJ}{d\tau} = 2\int_{\omega_a}^{\omega_b} \tau\left(F(\omega,\tau_{\sigma l})\right)^2 - Q_0^{-1}F(\omega,\tau_{\sigma l})\, d\omega = 0. \tag{3.7}$$

We can now solve for τ, and find,

$$\tau = \frac{1}{Q_0}\frac{\displaystyle\int_{\omega_a}^{\omega_b} F(\omega,\tau_{\sigma l})\, d\omega}{\displaystyle\int_{\omega_a}^{\omega_b} \left(F(\omega,\tau_{\sigma l})\right)^2\, d\omega}. \tag{3.8}$$

The two integrals in equation (3.8) can be solved analytically, which yields an explicit formula for τ. The integrands (or methods) can be found in any standard work on integral calculus or collection of mathematical formulas (e.g., Råde and Westergren [17]). It is of course possible to solve the integrals by some numerical method as well. The final formula for τ is,

$$\tau = \frac{1}{Q_0}\frac{\displaystyle\sum_{l=1}^{L} I_{0l}}{\displaystyle\sum_{l=1}^{L} I_{1l} + 2\sum_{l=1}^{L-1}\sum_{k=l}^{L} I_{2kl}}, \tag{3.9}$$

where

$$I_{0l} = \frac{1}{2\tau_{\sigma l}}\left[\log\left(1+\omega^2\tau_{\sigma l}^2\right)\right]_{\omega_a}^{\omega_b} \tag{3.10}$$

$$I_{1l} = \frac{1}{2\tau_{\sigma l}}\left[\arctan\left(\omega\tau_{\sigma l}\right) - \frac{\omega\tau_{\sigma l}}{1+\omega^2\tau_{\sigma l}^2}\right]_{\omega_a}^{\omega_b} \tag{3.11}$$

$$I_{2lk} = \frac{\tau_{\sigma l}\tau_{\sigma k}}{\tau_{\sigma k}^2 - \tau_{\sigma l}^2}\left[\frac{\arctan\left(\omega\tau_{\sigma l}\right)}{\tau_{\sigma l}} - \frac{\arctan\left(\omega\tau_{\sigma k}\right)}{\tau_{\sigma k}}\right]_{\omega_a}^{\omega_b}. \tag{3.12}$$

The τ-method generally yields a slightly too small τ, i.e., slightly too large Q, caused by the approximation $\tau \ll 1$. By using a slightly smaller Q_0 in equation (3.9) than desired, it is possible to find the τ which yields the desired Q. The effect of underestimating τ is more pronounced for a larger number of relaxation mechanisms and a lower Q. An example of the τ-method is shown in Figure 4.2, where five relaxation mechanisms have been used to find a Q approximately equal to 20. Hence we used a Q_0 approximately equal to 18 in equation (3.9) to calculate τ.

If several τ are to be calculated for an identical $\tau_{\sigma l}$ distribution and frequency intervals, but different Q_0, it suffices to calculate the integrals I_{0l}, I_{1l}, and I_{2lk} and corresponding sums once. This can be seen from equation (3.9) since the integrals are independent of Q_0. To determine a new τ it is thus sufficient to divide by a new Q_0.

The distribution of the $\tau_{\sigma l}$ is not determined by the τ-method. Distributing the $\tau_{\sigma l}$ logarithmically over the frequency range of interest generally yields good approximations to a constant Q. This is $\tau_{\sigma l} = 1/\omega_l$, about one per one-two octaves, which is a good *ad hoc* rule of thumb (cf., Liu et al. [10], Blanch et al. [2], and example in Figure 4.2 and Table 4.4). A closed formula for the optimal distribution of the $\tau_{\sigma l}$ is still an open question.

The use of a single parameter determining the magnitude of several SLSs also yields considerable savings for forward modeling of viscoelastic waves. There are both less memory and calculations required for a certain problem (see section *Implementation Considerations*).

4 Numerical Experiments

In this section we benchmark the τ-method against the Padé approximant method [7], a single relaxation mechanism (one SLS) approximation, and an analytical solution which we will start by deriving. We compare seismograms from 1-D finite-difference simulations using the method described by Robertsson et al. [16]. The results can immediately be generalized to 2-D and 3-D, since P- and S-waves are modeled independently. We use models with different attenuation as well as Q-approximations based on different numbers of relaxation mechansims (or SLS) to evaluate the different methods.

An analytical solution for anelastic wave propagation in a *homogeneous* medium may be obtained through the principle of correspondence [3]. From D'Alembert's solution we obtain the impulse response for the one-dimenstional case as,

$$\phi(\omega, x) = e^{-i\omega x/v(\omega)}, \tag{4.1}$$

where $i = \sqrt{-1}$, x is the offset from the initial location of the source, and,

$$v(\omega) = c(\omega)\left(1 + \frac{i}{2Q(\omega)} sgn(\omega)\right), \tag{4.2}$$

where $sgn(\omega) = -1$ for $\omega < 0$, and $sgn(\omega) = 1$ for $\omega > 0$. $c(\omega)$ and $Q(\omega)$ are the desired velocity and Q relations. An arbitrary source wavelet can thus be convolved with the impulse response in equation (4.1) to yield the solution as a function of offset and time, enabling the calculation of analytic seismograms for desired velocity and Q-relations as functions of frequency.

Futterman [8] proposed three different analytical expressions to model Q as a function of frequency in real earth media, based on experimental results by McDonal et al. [14]. All the models exhibit a constant Q except close to $0\,Hz$. The velocity vs. frequency relation is given from the Q vs. frequency relation through Kramer-Krönig's relation [8]. Martinez and McMechan [11] chose one of the expressions to obtain a τ-p domain solution for anelastic wave propagation. Using shale and Plexiglass, Wuenschel [19] showed that another of Futtermans [8] expressions fits very close to experimental results. This is the one we used to benchmark the different Q-modeling algorithms. The velocity is given by,

$$c(\omega) = c_0 / \left(1 - \frac{1}{2\pi Q_0} log \mid (\omega/\omega_0)^2 - 1 \mid\right), \tag{4.3}$$

and thus Q is,

$$Q(\omega) = Q_0 \left(1 - \frac{1}{2\pi Q_0} log \mid (\omega/\omega_0)^2 - 1 \mid\right). \tag{4.4}$$

ω_0 is a reference frequency, much smaller than the frequencies modeled. In our experiments we used ω_0=0.01 rad/s, but the value of ω_0 is not crucial for the model. c_0 is the reference velocity chosen to yield the desired velocity at the center frequency of the wavelet in the simulations, and Q_0 is the analogous reference Q-value. In our simulations we will refer to the velocity and the Q as the values at the center frequency of the wavelet used in the experiments (10 Hz).

4.1 Test case

The source in the simulations is a Ricker wavelet with an amplitude of 1 and a center frequency of 10 Hz, which yields a band width between 2 and 25 Hz for a 40 dB threshhold. Number of gridpoints and timestep for the viscoelastic simulation were chosen in accordance with rules outlined by Robertsson et al. [16]. The density, ρ, is 1000 kg/m^3, and c_0=1500 m/s. We chose two models. In the first we used a moderate value of Q_0=100. This is typical for shallow rocks or consolidated sediments (e.g., Bourbie et al. [4] and Hamilton [9]). In the second model Q_0=20, which is a low value characteristic of shallow unconsolidated sediments on the seafloor (e.g., Hamilton [9]). The receivers are located at 3000 m and 6000 m from the source, corresponding to 20 and 40 wavelengths for the center frequency of the wavelet.

4.1.1 Q-modeling

We investigated two cases. First, we employed five relaxation mechanisms to approximate the Q=20 model. For strong attenuation, accurate modeling of Q is naturally more crucial than for cases where the attenuation is weaker. We do not show results from approximations of a Q of 100 using five relaxation mechanisms since the excellent results we achived for the Q=20 approximation already illustrates the case of five relaxation mechanisms. Second, we employed two relaxation mechanisms to approximate both the Q=20 and the Q=100 models. As described above, we have constrained the distribution of $\tau_{\sigma l}$ so that for each of the Q-optimization methods, the $\tau_{\sigma l}$ are identical both for Q=100 and Q=20. This yields optimally low memory requirements, which is particularly important in 2-D and 3-D applications. The relaxation times obtained from the different Q-optimization methods are listed in Tables 4.1, 4.2, 4.3, 4.4, and 4.5.

l	$\tau_{\sigma l}$ (ms)
1	99.472
2	7.2343

Table 4.1: Optimized $\tau_{\sigma l}$ for two relaxation mechanisms to yield a constant Q between 2 and 25 Hz, using the τ-method. τ=0.10110 for Q=20, and τ=0.019156 for Q=100.

l	$\tau_{\sigma l}$ (ms)	$\tau_{\varepsilon l}$ (ms) (Q=20)	$\tau_{\varepsilon l}$ (ms) (Q=100)
1	5.7653	5.9428	5.7946
2	21.495	23.471	21.882

Table 4.2: Optimized relaxation mechanisms (for a total of two) to yield a constant Q between 2 and 25 Hz, using the Padé approximant method.

Equation (2.11) may be used to calculate Q as a function of frequency for the different Q-optimization methods. In Figure 4.1 we have plotted these curves when using two relaxation mechanisms to approximate a Q of 20 between 2 and 25 Hz. As we can see the τ-method yields a close to constant Q over the entire frequency band. The single relaxation mechanism approximation yields a Q that roughly varies between 18 and 30. The chosen source wavelet has its energy concentrated around 10 Hz, and since the single relaxation mechanism approximation varies between a Q of 18 and 22 between 5 and 20 Hz, we can expect fairly good simulation results also for this optimally computational inexpensive Q-modeling method. The Padé approximant method yields a quite poor result, barely better than the single relaxation mechanism approximation. The Padé approximant method is in some sense optimal, but converges slowly as the number of approximants are increased, when a constant-Q over a relatively short frequency band is desired.

In Figure 4.2 we show the Q-approximations when using five mechanisms to approximate a Q of 20 between 2 and 25 Hz. The τ-method yields very close to constant Q over the frequency band. Also, the Padé approximant method now gives a much better approximation compared to the case when using only two approximants. It is however still worse than the approximation obtained through the τ-method.

In Figure 4.3 we illustrate the Q-approximations when using two mechanisms to approximate a Q of 100 between 2 and 25 Hz. Again, the τ-method yields the best result and the Padé approximant

τ_{σ} (ms)	τ_{ε} (ms) (Q=20)	τ_{ε} (ms) (Q=100)
15.056	16.824	15.374

Table 4.3: Optimized relaxation mechanism to yield a constant Q between 2 and 25 Hz, for a single relaxation mechanism.

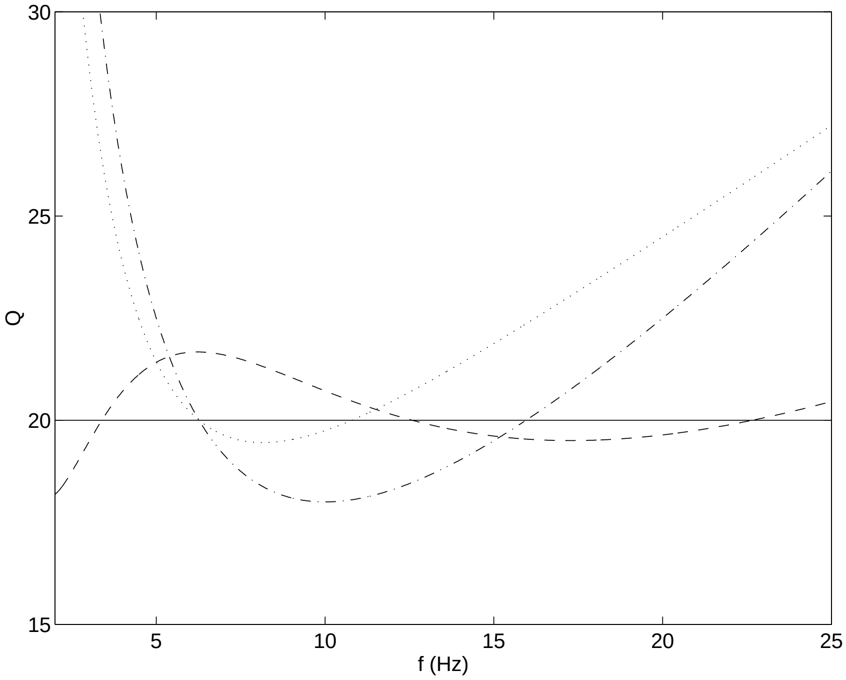

Figure 4.1: Approximations to a constant Q of 20 between 2 and 25 Hz. $Q_0 \approx 18$ in algorithm. Solid: Desired Q. Dashed: τ-method using two relaxation mechanisms. Dotted: Padé approximant method using two relaxation mechanisms. Dash-dotted: Single relaxation mechanism approximant.

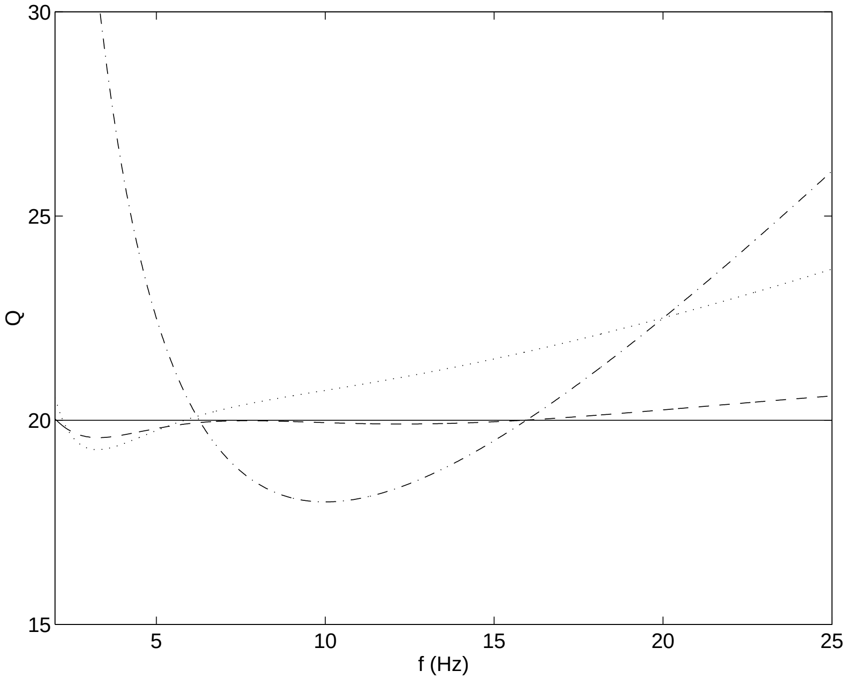

Figure 4.2: Approximations to a constant Q of 20 between 2 and 25 Hz. $Q_0 \approx 18$ in algorithm. Solid: Desired Q. Dashed: τ-method using five relaxation mechanisms. Dotted: Padé approximant method using five relaxation mechanisms. Dash-dotted: Single relaxation mechanism approximant.

l	$\tau_{\sigma l}$ (ms)
1	265.26
2	52.203
3	10.273
4	2.0218
5	0.39789

Table 4.4: Optimized $\tau_{\sigma l}$ for five relaxation mechanisms to yield a constant Q between 2 and 25 Hz, using the τ-method. τ=0.060168 for Q=20.

l	$\tau_{\sigma l}$ (ms)	$\tau_{\varepsilon l}$ (ms) $(Q$=20$)$
1	1.1132	1.1265
2	1.3792	1.4033
3	2.1214	2.1748
4	4.5928	4.7730
5	22.466	24.341

Table 4.5: Optimized relaxation mechanisms (for a total of five) to yield a constant Q between 2 and 25 Hz, using the Padé approximant method.

method yields a result similar to that of the single relaxation mechanism approximation.

4.1.2 Simulations

In Figure 4.4 we have plotted the seismograms collected at 6000 m offset when approximating a constant Q of 100 with two relaxation mechanisms. As we can see all methods reproduce the analytic solution fairly well, although the τ-method clearly is the most successful. The Padé approximant method and the single relaxation mechanism approximation both yield worse but reasonably accurate and similar solutions. The latter is not a surprise since the corresponding Q vs. frequency relations are very similar (see Figure 4.3).

In Figure 4.5 we show the seismograms collected at 3000 m offset when approximating a constant Q of 20 using two relaxation mechanisms. All methods display highly accurate results, even though the τ-method again is most successful. In Figure 4.6 we show the analogous seismograms collected at 6000 m offset. Notice that the amplitude of the analytic solution now only is approximately 1 percent of the initial amplitude. Furthermore, for 40 wavelengths path of propagation, cylindrical and spherical spreading would significantly contribute to even stronger decay of the waveform in 2-D and 3-D simulations. There are few seismic applications, if any, where accurate modeling of such extreme cases is of interest. We achive a highly accurate solution using the τ-method with only two relaxation mechanisms. The Padé approximant method as well as the single relaxation mechanism approximation yield less accurate results. The single relaxation mechanism is however

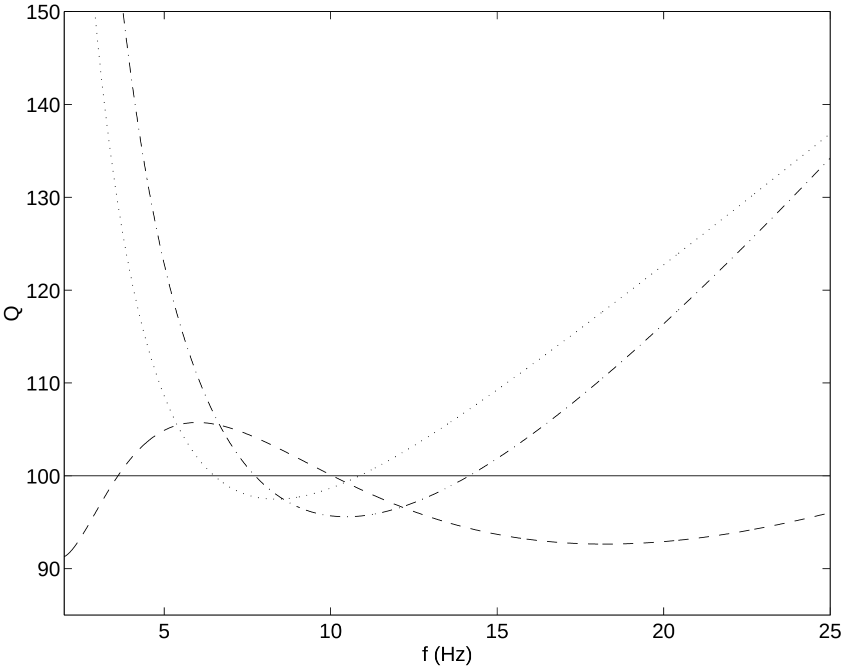

Figure 4.3: Approximations to a constant Q of 100 between 2 and 25 Hz. $Q_0 \approx 95$ in algorithm. Solid: Desired Q. Dashed: τ-method using two relaxation mechanisms. Dotted: Padé approximant method using two relaxation mechanisms. Dash-dotted: Single relaxation mechanism approximant.

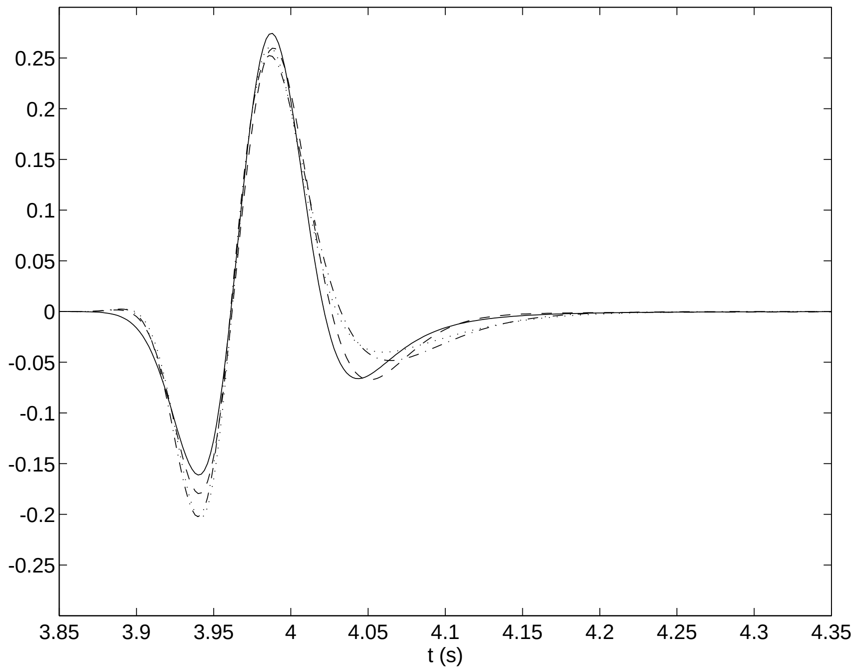

Figure 4.4: Seismograms collected at 6000 m offset in the model with a constant Q of approximation of 100 between 2 and 25 Hz. Solid: Analytical solution. Dashed: τ-method using two relaxation mechanisms. Dotted: Padé approximant method using two relaxation mechanisms. Dash-dotted: Single relaxation mechanism approximant.

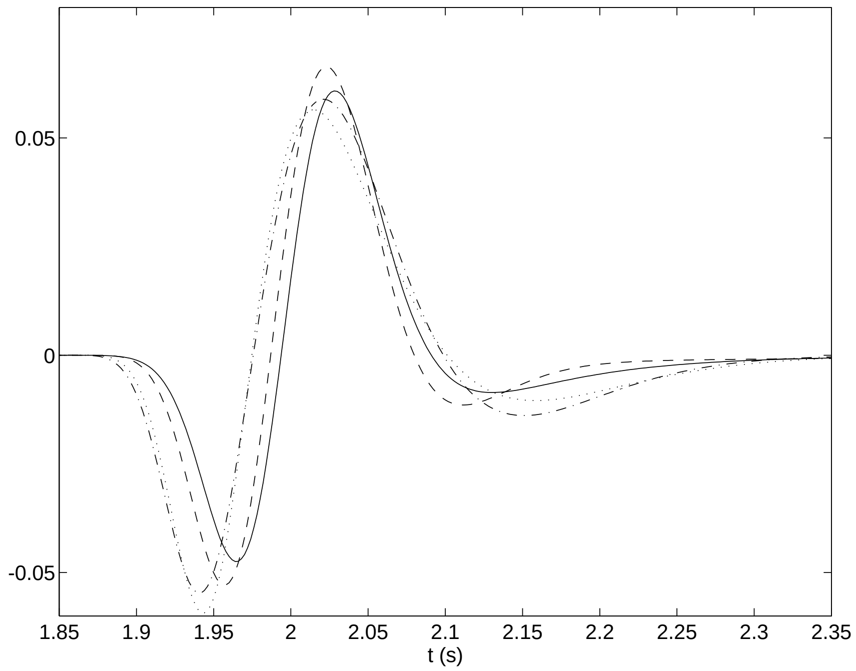

Figure 4.5: Seismograms collected at 3000 m offset in the model with a constant Q of approximation of 20 between 2 and 25 Hz. Solid: Analytical solution. Dashed: τ-method using two relaxation mechanisms. Dotted: Padé approximant method using two relaxation mechanisms. Dash-dotted: Single relaxation mechanism approximant.

the trivial and always least computationally expensive constant Q approximation. We find it remarkable that such a simple approximation yields a for most applications sufficiently accurate result after 40 wavelengths propagation of a Ricker wavelet through a medium with a Q of 20. Since most high frequency components are attenuated, the seismograms we collect at 6000 m offset is reflected by the character of the Q vs. frequency curves at lower frequencies (somewhere around 5 Hz). These components were much weaker in the original wavelet but are not subjected to as strong attenuation due to the fewer wavelengths in the path of propagation.

Finally we show the results when using five relaxation mechanisms to approximate a constant Q of 20. At 3000 m offset (Figure 4.7), the analytic solution is well reproduced by all methods, as was the case in Figure 4.5 when using only two relaxation mechanisms. Again, the τ-method yields the most accurate reult. In Figure 4.8 we show seismograms collected at 6000 m offset. The τ-method yields an excellent result; The collected seismogram is very close to the analytic solution for this the most extreme case of strong attenuation and long path of propagation. As is evident from Figure 4.2, the method models wave propagation just as well over the entire frequency band between 2 and 25 Hz. The practically inconvenient and expensive Padé approximant method yields a quite poor result, only marginally more accurate than the single relaxation mechanism

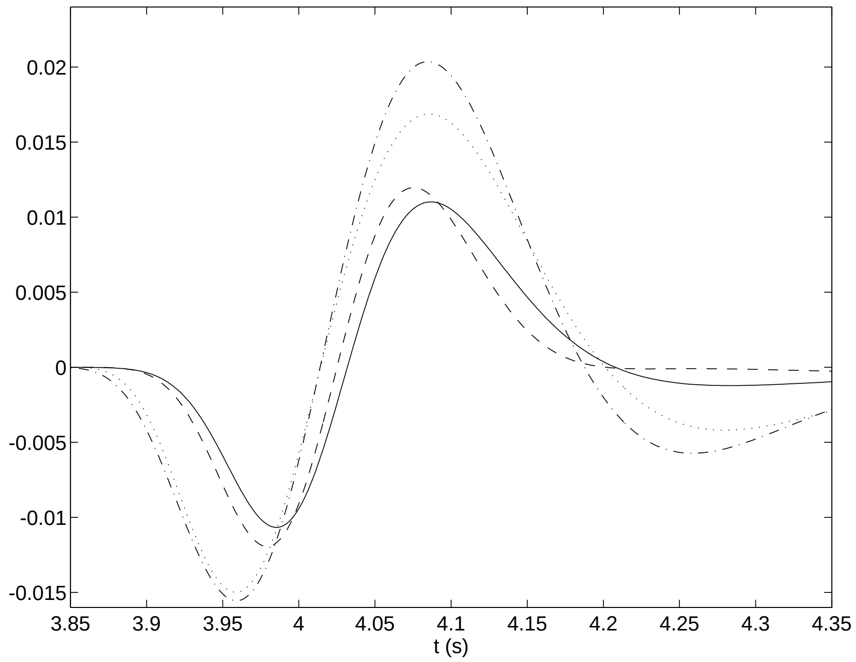

Figure 4.6: Seismograms collected at 6000 m offset in the model with a constant Q of approximation of 20 between 2 and 25 Hz. Solid: Analytical solution. Dashed: τ-method using two relaxation mechanisms. Dotted: Padé approximant method using two relaxation mechanisms. Dash-dotted: Single relaxation mechanism approximant.

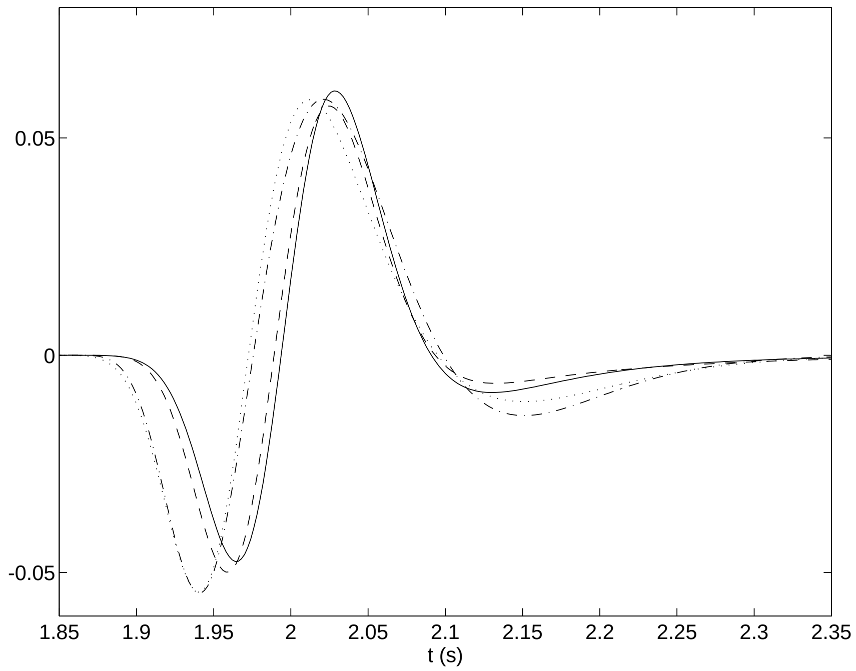

Figure 4.7: Seismograms collected at 3000 m offset in the model with a constant Q of approximation of 20 between 2 and 25 Hz. Solid: Analytical solution. Dashed: τ-method using five relaxation mechanisms. Dotted: Padé approximant method using five relaxation mechanisms. Dash-dotted: Single relaxation mechanism approximant.

approximation.

5 Implementation Considerations

Modelling of viscoelastic wave propagation has been regarded as considerably more computationally expensive than purely elastic wave propagation. Robertsson et al. [16] presented a highly efficent viscoelastic finite-difference scheme enabling modeling of widely varying Q in highly heterogeneous media. 2-D as well as 3-D schemes have been implemented at a computational cost that only marginally exceeds that of analogous purely elastic finite-difference schemes [16]. Computational efficiency may be stated in terms of the number of parameter and variable fields that are required to be stored simultaneously and the number of calculations per grid-point and time step required for a particular scheme. In Table 5.1 we compare the computational efficiency for 2-D and 3-D viscoelastic schemes using the different Q-modeling algorithms to the analogous elastic schemes. Both the memory requirements and the number of calculations are very much dependent on the Q-modeling algorithm employed. From Table 5.1 we conclude that the τ-method is superior to

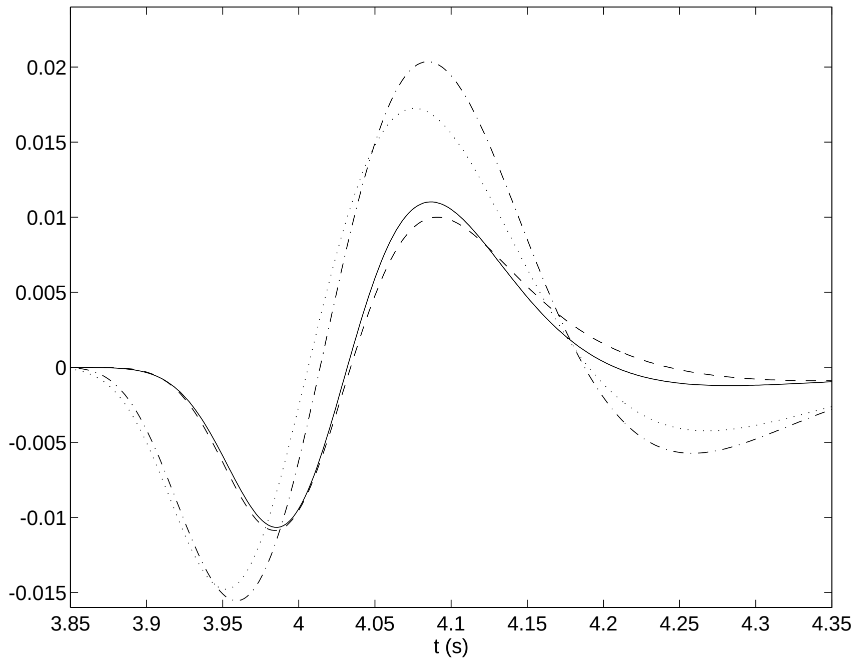

Figure 4.8: Seismograms collected at 6000 m offset in the model with a constant Q of approximation of 20 between 2 and 25 Hz. Solid: Analytical solution. Dashed: τ-method using five relaxation mechanisms. Dotted: Padé approximant method using five relaxation mechanisms. Dash-dotted: Single relaxation mechanism approximant.

Method	Memory (2-D)	Calculations (2-D)	Memory (3-D)	Calculations (3-D)
Single mech.	13	120	20	220
τ 2 mech.	16	130	26	240
τ 5 mech.	25	170	44	310
Padé 2 mech.	18	140	28	255
Padé 5 mech.	33	200	52	360
Elastic	8	70	12	160

Table 5.1: The computational efficiency of viscoelastic finite-difference schemes as [16] implemented them when employing the different Q-modeling methods, compared to the analogous purely elastic finite-difference schemes. The computational efficiency is characterized by the number of parameter or variable fields required to be stored simultaneously and by the number of calculation per gridpoint and time step necessary.

the Padé approximant method also when it comes to computational efficiency. The simplest Q-modeling method, the single relaxation mechanism approximation, is only marginally more expensive than purely elastic modelling.

As we have seen the single relaxation mechanism approximation yields results that are sufficiently accurate for most practical purposes. Q is a physical quantity that is difficult to measure with high accuracy in real earth media [18]. Also, it is still debated how realistic a constant Q as a function of frequency model always is [4]. Thus, the uncertainty of the modeling may very well be greater than the inaccuracy of a single relaxation mechansim constant Q approximation. There is however another reason for using more than one relaxation mechanisms. Absorbing boundaries can be implemented by decreasing the attenuation to as low as Q=2 within a narrow frame around the desired grid [16]. To avoid impedance reflections it is important to tune the Lamé parameters for constant velocity. The deviation from a constant Q for such low values of Q is greater than for the more physically realistic values of Q within the desired grid, leading to velocity variations within the frequency band of interest in the absorbing frame. Compensation may thus only be achived by employing additional relaxation mechanisms for a closer to constant Q in the absorbing region. For a wavelet with a frequency content similar to that of the Ricker wavelet, we found that two relaxation mechanisms yield sufficiently constant Q in the absorbing frame.

6 Conclusions

We have outlined the methodology of an algorithm, the τ-method, to model constant Q vs. frequency for viscoelastic/viscoacoustic wave propagation simulators. The τ-method enables considerable savings of memory and computations for both 2-D and 3-D viscoelastic finite-difference schemes and is much easier to implement compared to other methods, such as the Padé approximant method [7]

We performed a series of 1-D experiments to compare the τ-method to an analytical solution based on the principle of correspondence [3] and a constant-Q model by Futterman [8]. We also compared the method to the Padé approximant method and a single relaxation mechanism approximation. We found that the τ-method also yields the highest accuracy in the simulations. The Padé approximant method should however yield the most accurate results for cases with large numbers (probably at least 10) of SLSs [7].

The single relaxation mechanism approximation produced reasonably accurate results. For most applications this method yields sufficiently accurate modeling of Q. In practice, we see no reason for employing more accurate approximations than the τ-method using two relaxation mechanisms. This method also enables implementation of highly efficient absorbing boundaries.

7 Acknowledgments

This work was supported by ONR grants N00014-89-J3015 and N00014-89-J1115, the Schlumberger Foundation, and The Rice Inversion Project. TRIP Sponsors for 1994 are: Advance Geophysical, Amoco Production Co., Conoco Inc., Cray Research Inc., Exxon Production Research Co., Interactive Network Technologies, Mobil Research and Development Corp., and Texaco Inc. . The numerical experiments were performed on the IBM RS-6000/580 at the Geophysical Computing Center of Rice University.

References

[1] Blanch, J. O., and Symes, W. W., 1994, Linearized inversion in viscoelastic media: *in* Diachok, O,. Caiti, A,. Gerstoft, P., and Schmidt, H., Eds., Full Field Inversion Methods in Ocean and Seismic Acoustics: Kluwer Academic Publishers, (To appear).

[2] Blanch, J. O., Robertsson, J. O. A., and Symes, W. W., 1993, Viscoelastic finite difference modeling: Technical Report 93-04, Department of Computational and Applied Mathematics, Rice University.

[3] Bland, D. R., 1960, The theory of linear viscoelasticity: Pergamon Press.

[4] Bourbie, T., Coussy, O., and Zinzner, B., 1987, Acoustics of porous media: Gulf Publishing Company.

[5] Carcione, J. M., Kosloff, D., and Kosloff, R., 1988, Wavepropagation simulation in a linear viscoacoustic medium: Geophys. J. Roy. Astr. Soc., **93**, 393-407.

[6] Christensen, R. M., 1982, Theory of viscoelasticity - An introduction: Academic Press Inc.

[7] Day, S. M., Minster, J. B., 1984, Numerical simulation of attenuated wavefields using a Padé approximant method: Geophys. J. R. Astr. Soc., **78**, 105–118.

[8] Futterman, W. I., 1962, Dispersive body waves: J. Geophys. Res., **67**, 5279–5291.

[9] Hamilton, E. L., 1980, Geoacoustic modeling of the seafloor: J. Acoust. Soc. Am., **68**, 1313–1340.

[10] Liu, H. P., Anderson, D. L., and Kanamori, H., 1976, Velocity dispersion due to anelasticity: implications for seismlogy and mantle composition: Geophys. J. Roy. Astr. Soc., **47**, 41-58.

[11] Martinez, R. D., and McMechan, G. A., 1991a, τ-p seismic data for viscoelastic media - Part 1: Modelling: Geophys. Prosp., **39**, 141-156.

[12] Martinez, R. D., and McMechan, G. A., 1991b, τ-p seismic data for viscoelastic media - Part 2: Linearized Inversion: Geophys. Prosp., **39**, 157-181.

[13] Martinez, R. D., 1993, Wavepropagation effects on amplitude variation with offset measurements: A modeling study: Geophysics, **58**, 534-543.

[14] McDonal, F., J., Angona, F., A., Mills, R., L., Sengbush, R., L., van Nostrand, R., G., White, J., E., 1958, Attenuation of shear and compressional waves in Pierre shale: Geophysics, **23**, 421-439.

[15] Pipkin, A. C., 1986, Lectures on viscoelasticity theory: Springer Verlag.

[16] Robertsson, J. O. A., Blanch, J. O., and Symes, W. W., 1994, Viscoelastic finite-difference modeling: Accepted for publication in Geophysics.

[17] Råde, L., and Westergren, B., 1988, BETA β Mathematics Handbook: Studentlitteratur.

[18] White, R. E., 1992, Short note: The accuracy of estimating Q from seismic data: Geophysics, **57**, 1508–1511.

[19] Wuenschel, P. C., 1965, Dispersive body waves – an experimental study: Geophysics, **30**, 539–551.